When the "exact" discrete gradient is not the best choice in optimal shape design?

Alfonso Bueno-Orovio*
Oxford University, Oxford OX1 3QD, UK, and Polytechnic University of Madrid, Madrid 28040, Spain
Carlos Castro†
Polytechnic University of Madrid, Madrid 28040, Spain
Karthikeyan Duraisamy‡, Francisco Palacios§
Stanford University, Stanford CA 94305, USA
Enrique Zuazua¶
Basque Center for Applied Mathematics, Derio 48160, Spain

In aerodynamics, Optimal Shape Design (OSD) aims to find the minimum of an objective function describing an aerodynamic property, by controlling the Partial Differential Equation (PDE) modeling the dynamics of the flow that surrounds an aircraft.

The objective function minimization is usually achieved by means of an iterative process which requires the computation of the gradients of the cost function with respect to the design variables. Gradients can be computed in a variety of ways but, to the best of our knowledge, the most efficient method to compute the cost function gradient is the so-called "adjoint method".

At the computational level there are two approaches to the adjoint system: the continuous method and the discrete one. In the continuous approach, the adjoint equations are derived from the flow equations and then subsequently discretized (continuous adjoint methodology[1,2]), whereas in the discrete approach the adjoint equations are directly derived from the discretized governing equations (discrete adjoint,[3] automatic differentiation,[4] finite differences[5] or complex step[6] methodologies).

In the aeronautical practice, the target is to minimize a discrete objective function and, consequently, the "discrete approach" seems to be more "natural". However, as shown in this paper, there are relevant situations (strong shock waves or wrong numerical grid orientation) in which the gradient obtained using a discrete approach shows a non-physical oscillatory behavior. In those cases, the discrete objective function (at the smallest scales) fails to capture the behavior of the continuous objective function and, consequently, the discrete approach to compute the objective function gradient could be inappropriate.

In this article, we will analyze the origin of the aforementioned numerical oscillations in different systems (Burgers' equation, quasi 1D Euler's equations and 2D Euler's equations). Some numerical experiments will be shown and their impact on the optimization process will be explained. Finally some conclusions and further recommendation will be presented.

I. Introduction to optimal shape design

AERODYNAMIC applications of optimal shape design involve systems governed by PDEs formulated on a fluid domain Ω, containing air delimited by disconnected boundaries divided into a "far field" Γ_∞ and some solid wall boundaries S (airplane surfaces).

*Research Assistant, Computing Laboratory, Computational Biology Group, and Departamento de Matemáticas e Informática, ETSI Caminos, Canales y Puertos.
†Professor, Departamento de Matemáticas e Informática, ETSI Caminos, Canales y Puertos.
‡Consulting Assistant Professor, Department of Aeronautics and Astronautics.
§Engineering Research Associate, Department of Aeronautics and Astronautics, AIAA Member.
¶Ikerbasque Research Professor & Scientific Director, Basque Center for Applied Mathematics (BCAM).

We will restrict ourselves to the analysis of optimization problems involving objective functions J defined on the solid wall S, whose value depends on the conservative flow variables U obtained from the solution of the Euler's equations. In this context, a generic optimization problem can be stated as follows: find $S_{\min} \in \mathcal{S}_{ad}$ such that

$$J(S_{\min}) = \min_{S_{\min} \in \mathcal{S}_{ad}} J(S), \tag{1}$$

where $\mathcal{S}_{ad}$ is the set of admissible boundary geometries and

$$J(S) = \int_S j(P, \vec{n}_S)\, ds, \tag{2}$$

is the objective function, where $j(P, \vec{n}_S)$ is a smooth function which depends on $\vec{n}_S$ (inward-pointing unit vector normal to S) and the pressure P which is computed as a nonlinear combination of the conservative flow variables U.

In the engineering practice instead of computing the exact continuous objective function one computes a discrete approximation in which the time and physical domain is discretized. The objective function is evaluated by means of a discrete integration rule and P is estimated by means of a numerical approximation scheme for solving the Euler's equations which provides $P_{\Delta x}$.

A key element of the optimization technique is the evaluation of the gradient of $J(S)$ (continuous approach) or the gradient of $J_{\Delta x}(S)$ (discrete approach). In principle, the discrete approach seems a more natural choice. But, some difficulties[7,8] arise when $J_{\Delta x}$ shows some fluctuations due to the nature of the numerical scheme.

The objective of this paper is to point at and analyze some circumstances in which the use of an "exact" discrete approach to compute the gradient of an aerodynamic objective function is not adequate (in particular at zones where there are strong shocks or where the numerical grid is not well oriented). In the next sections evidences of this behaviour will be shown in the frame of Burgers' equation, and Euler's equations (quasi 1D and 2D).

II. Systems governed by the Burgers' equation

Burgers' equation has been chosen as the first reference model of this article because it has a nonlinear flux term identical to the convection term of the Euler's equations, being for that reason representative for the non-linearities occurring in the flow equations.

In this section we will consider two problems, the classical unsteady inviscid Burgers' problem with a discontinuous initial data, and a modified version of inviscid Burgers' equation with a source term, to obtain a steady state solution[9] similar to some transonic results in quasi-1D Euler's problems.

Unsteady Problem. The inviscid Burgers' problem. We consider the system

$$\begin{cases} \partial_t u + \partial_x \left(\frac{u^2}{2}\right) = 0, & -\infty < x < \infty, \quad 0 < t < T, \\ u(x,0) = u^0_\beta(x), & -\infty \le x \le \infty, \end{cases} \tag{3}$$

where

$$u^0_\beta(x) = \begin{cases} 1 & \text{if } -\infty < x \le 0, \\ -1+\beta & \text{if } 0 < x \le \infty. \end{cases} \tag{4}$$

and the parameter $\beta \in (0, 0.2)$. Let us take two different objective functions depending on β,

$$J^L(\beta) = \int_{-2}^{2} u_\beta(x,T)\, dx, \quad \text{and } J^Q(\beta) = \int_{-2}^{2} u^2_\beta(x,T)\, dx, \tag{5}$$

where $u_\beta(x,t)$, is the unique entropy solutions of (3). Note that the solutions of (3) can be obtained from the initial data by using characteristics. As the objective functions depend on the solution in the interval $(-2,2)$, only the characteristcs entering in this interval at time $t = T$ are relevant for the optimization problem. It is well-known that, in this case, characteristics are straight lines whose slope depend on the value of the solution at the point where they pass through. For the given initial data the solution is

$$u(x,t) = \begin{cases} 1 \text{ if } x \in (-\infty, \beta t/2), \\ -1+\beta \text{ if } x \in (\beta t/2, \infty), \end{cases} \tag{6}$$

and it has a discontinuity at $x = \beta t/2$, for each $t \in [0, T]$. Therefore, the slope of the characteristis is 1 to the left of the shock and $-1 + \beta$ to the right. This means that only the values of the initial datum in $(-2 - T, 2 + T(1 - \beta))$ are relevant to compute $u(x, T)$ in $x \in (-2, 2)$.

Steady Problem. The inviscid Burgers' equation with a source term,

$$\begin{cases} \partial_t v + \partial_x \left(\frac{v^2}{2}\right) = \partial_x(\frac{\sin^2 x}{2}), & 0 \le x \le \pi, \quad 0 < t < \infty, \\ v(0,t) = v(\pi,t) = 0, & 0 < t < \infty, \\ v(x,0) = v^0_\beta(x) = \beta \sin(x), & 0 < x < \pi, \end{cases} \tag{7}$$

where $0.7 < \beta < 0.8$. The analytical solution of this problem is:

$$v_\infty(x,\beta) = \lim_{t\to+\infty} v(x,\beta,t) = \begin{cases} v^+ = \sin x, & 0 < x < X_S \\ v^- = -\sin x, & X_S < x < \pi \end{cases} \tag{8}$$

where the shock position $X_S = \pi - \sin^{-1}(\sqrt{1-\beta^2})$ is a function of the parameter β in the initial condition.

On the other hand, we will also consider two objective functions defined by

$$J^L(\beta) = \int_0^\pi v_\beta(x,\infty)\,dx, \quad \text{and } J^Q(\beta) = \int_0^\pi v^2_\beta(x,\infty)\,dx, \tag{9}$$

where $v_\beta(x,t)$ is the unique entropy solutions of (7), and $v_\beta(x,\infty) = \lim_{t\to+\infty} v_\beta(x,t)$.

A. Objective function gradient using the continuous adjoint strategy

In this section we show how classical adjoint calculus can be used to compute the derivative of the functionals in (5) and (9) with respect to β. Note that the parameter β only affects the initial condition in (4) and (7). Therefore it is natural to see perturbations in the parameter β as a particular case of a general perturbation of the initial condition δu^0 or δv^0.

Therefore it is natural to see the variation of this parameter as a particular case of a general perturbation of the initial condition δu^0, which is a smooth function with a discontinuity at $x = 0$.

In general, these functions can be perturbed in two ways: by considering smooth variations of $u^0(x)$ to both sides of the discontinuity, or by perturbing the position of the discontinuity itself $x = \varphi^0$. In this way, any perturbation $u^{0,\varepsilon}$ of u^0 can be written as

$$u^{0,\varepsilon}(x) = u^0(x) + \varepsilon\delta u^0(x) - [u]_{\varphi_0}\chi_{[\varphi^0,\varphi^0+\varepsilon\delta\varphi^0]} + o(\varepsilon),$$

where $\chi_{[a,b]}$ is the characteristic function of the interval $[a, b]$,

$$\chi_{[a,b]}(x) = \begin{cases} 1 \text{ if } x \in [a,b], \\ 0 \text{ elsewhere.} \end{cases} \tag{10}$$

Thus, any perturbation $u^{0,\varepsilon}$ may be described, to first order, by the pair $(\delta u^0(x), \delta\varphi^0)$.

Unsteady Problem. Note that the solution of (3) has a discontinuity along a curve $x = \varphi(t)$. Thus, the above description for the perturbation of a discontinuous function u^0 applies also to the solution $u(x,t)$ of (3) for all $t > 0$. In particular, a perturbation of the initial datum $u^{0,\varepsilon}$ will provide a solution $u^\varepsilon(x,t)$ that, at first order, can be described by the pair $(\delta u(x,t), \delta\varphi(t))$, for al time $t > 0$.

In this case, the variation of the functionals are given by

$$\delta J^L = \int_{-2}^2 \delta u(x,T)\,dx - [u]_{\varphi(T)}\delta\varphi(T), \quad \text{and } \delta J^Q = \int_{-2}^2 2u(x,T)\delta u(x,T)\,dx - [u^2]_{\varphi(T)}\delta\varphi(T), \tag{11}$$

where the pair $(\delta u, \delta\varphi)$ satisfies

$$\begin{cases} \partial_t\delta u + \partial_x(u\delta u) = 0, & x \in (-\infty,\varphi(t)) \cup (\varphi(t),\infty), \quad 0 < t < T, \\ \delta u(x,0) = \delta u^0(x), & -\infty \le x \le \infty, \\ \delta\varphi'[u]_{\varphi(T)} + \varphi'[u_x]_{\varphi(T)}\delta\varphi & \\ \quad +\varphi'[\delta u]_{\varphi(T)} - [u_x u]_{\varphi(T)}\delta\varphi - [u\delta u]_{\varphi(T)} = 0, & 0 < t < T, \\ \delta\varphi(0) = \delta\varphi^0 \end{cases} \tag{12}$$

where $\delta\varphi^0$ is the perturbation in the position of the discontinuity for the initial datum.

Following a classical adjoint approach we can write

$$\delta J^L = \int_{-\infty}^{\infty} \delta u^0(x) p^L(x,0)\,dx + \delta\varphi^0 q^L(0), \quad \text{and } \delta J^Q = \int_{-\infty}^{\infty} \delta u^0(x) p^Q(x,0)\,dx + \delta\varphi^0 q^Q(0), \tag{13}$$

where the pairs (p^L, q^L) and (p^Q, q^Q) are solutions of the adjoint system

$$\begin{cases} -\partial_t p - u\partial_x p = 0, & x \in (-\infty, \varphi(t)) \cup (\varphi(t), \infty), \quad 0 < t < T \\ q(t) - p(\varphi(t), t) = 0, & 0 < t < T \\ p(x,T) = p^T(x), & x \in (-\infty, \varphi(t)) \cup (\varphi(t), \infty) \\ q(t) = q(T) = q^T, & 0 < t < T \end{cases} \tag{14}$$

corresponding to the final datum

$$\begin{aligned} \big(p^L(x,T), q^L(T)\big) &= (\chi_{[-2,2]}(x), 1), \\ \big(p^Q(x,T), q^Q(T)\big) &= \left(2u(x,T)\chi_{[-2,2]}(x), \frac{[u^2]_{\varphi(T)}}{[u]_{\varphi(T)}}\right), \end{aligned}$$

respectively.

For the particular perturbation u^0_β in (4), we have

$$\delta u^0 = \chi_{[0,4]}(x), \qquad \delta\varphi^0 = 0, \qquad p(x,0) = \chi_{[-2-T,2+T]}(x), \tag{15}$$

and therefore

$$\frac{dJ^L}{d\beta} = \int_0^{2+T} dx = 2 + T. \tag{16}$$

Steady Problem. Note that the solution of (7) has also a discontinuity along a curve $x = \varphi(t)$. This discontinuity, however, is not in the initial datum, but is generated at a later time $t = T_0$. In this case, the variation of the functionals are given by

$$\delta J^L = \int_0^{\pi} \delta v(x,\infty)\,dx - [v]_{\varphi(T)}\delta\varphi(T), \quad \text{and } \delta J^Q = \int_0^{\pi} 2v(x,\infty)\delta v(x,\infty)\,dx - [v^2]_{\varphi(T)}\delta\varphi(T), \tag{17}$$

where the pair $(\delta v, \delta\varphi)$ satisfies

$$\begin{cases} \partial_t \delta v + \partial_x (v\delta v) = 0, & x \in (0, \varphi(t)) \cup (\varphi(t), \pi), \quad T_0 < t < T, \\ \partial_t \delta v + \partial_x (v\delta v) = 0, & x \in (0, \pi), \quad 0 < t < T_0, \\ \delta v(0,t) = \delta v(\pi, t) = 0, & 0 < t < T, \\ \delta v(x,0) = \delta v^0(x), & 0 \le x \le \pi, \\ \delta\varphi'[v]_{\varphi(T)} + \varphi'[v_x]_{\varphi(T)}\delta\varphi & \\ \quad + \varphi'[\delta v]_{\varphi(T)} - [v_x v]_{\varphi(T)}\delta\varphi - [v\delta v]_{\varphi(T)} = 0, & T_0 < t < T, \end{cases} \tag{18}$$

where $\delta\varphi^0$ is the perturbation in the position of the discontinuity for the initial datum.

Following a classical adjoint approach we can write

$$\delta J^L = \int_0^{\pi} \delta u^0(x) p^L(x,0)\,dx, \quad \text{and } \delta J^Q = \int_0^{\pi} \delta u^0(x) p^Q(x,0)\,dx, \tag{19}$$

where the pairs (p^L, q^L) and (p^Q, q^Q) are solutions of the adjoint system

$$\begin{cases} -\partial_t p - u\partial_x p = 0, & x \in (0, \varphi(t)) \cup (\varphi(t), \pi), \quad 0 < t < T, \\ q(t) - p(\varphi(t), t) = 0, & T_0 < t < T \\ p(x,T) = p^T(x), & x \in (0, \varphi(t)) \cup (\varphi(t), \pi) \\ q(t) = q(T) = q^T, & T_0 < t < T \end{cases} \tag{20}$$

corresponding to the final datum

$$\begin{aligned}\left(p^L(x,T),q^L(T)\right) &= (1,1),\\ \left(p^Q(x,T),q^Q(T)\right) &= (2u(x,T),\frac{[u^2]_{\varphi(T)}}{[u]_{\varphi(T)}}),\end{aligned}$$

respectively. It is important to note that, in this particular case, as we know the analytical solution it is not necessary to use the adjoint strategy to compute the functional gradient.

Note that boundary conditions are not required in (20) due to the fact that characteristics do not meet the boundary of the domain.

B. Numerical tests using quadratic objective functions

In this section we will check that quadratic objective functions are not appropriated for a discrete approach in the gradient computation. As toy model we will use the steady state problem 7. Using the analytical solution it is possible to compute the value and gradient of the following quadratic objective function:

$$J^Q(\beta)=\int_0^\pi \frac{1}{2}u_\infty^2(x,\beta)\,dx=\int_0^\pi \frac{1}{2}\sin^2(x)\,dx=\frac{1}{4}x-\frac{1}{8}\sin(2x)|_0^\pi=\frac{1}{4}\pi,\ \text{and}\ \frac{\partial J^Q}{\partial\beta}=0 \tag{21}$$

In figure 1 the solution of the Burgers' equation is shown for $\beta=0.75$ and $\beta=0.755$. Note that, due to the 3 points representation of the shock there is an important difference between the analytical and the discrete solution at the shock location.

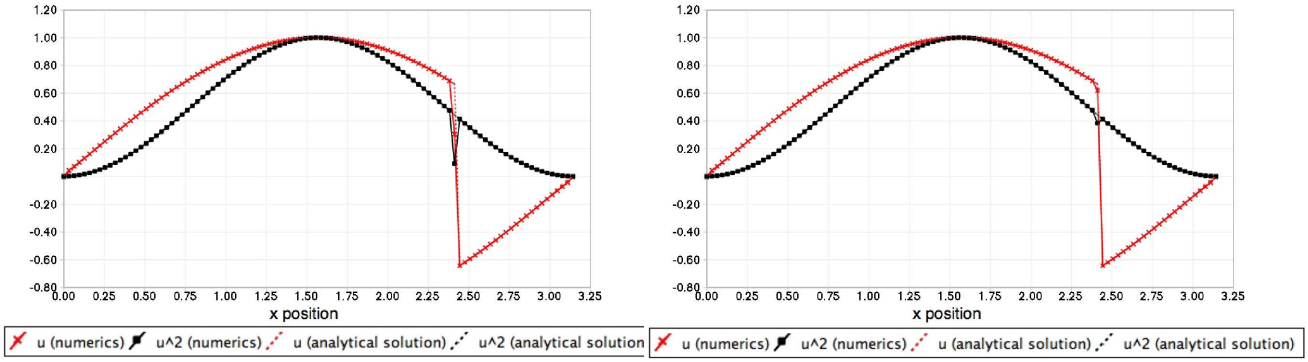

Figure 1. Discrete (continuous line) and analytical (dotted line) solution of steady Burgers' equations (black line) and square of the solution (red line) for $\beta=0.75$ (left) and $\beta=0.755$ (right).

In figure 2 (left) there is a comparison between the analytical value of the objective function and the discrete objective functions for different values of β. Finally, In figure 2 (right) the gradient computed with an "exact" discrete gradient methodology (forward finite differences) is shown.

III. Systems governed by the quasi 1D Euler's equations

In this section we consider a fluid moving through a duct of variable cross sectional area $h(x)$ and finite length. The dynamics of the fluid is governed by the quasi-one-dimensional Euler equations, that may be written as

$$\begin{cases}\frac{\partial}{\partial t}(hU)+\frac{\partial}{\partial x}(hF)-\frac{dh}{dx}Q=0 & \text{on } a<x<b,\\ U(x,0)=U_0(x), & \text{on } a<x<b,\\ +\text{ boundary conditions at } a \text{ and } b\end{cases} \tag{22}$$

or, for the steady state, as

$$\begin{cases}\frac{d}{dx}(hF)-\frac{dh}{dx}Q=0 & \text{on } a<x<b,\\ +\text{ boundary conditions at } a \text{ and } b\end{cases} \tag{23}$$

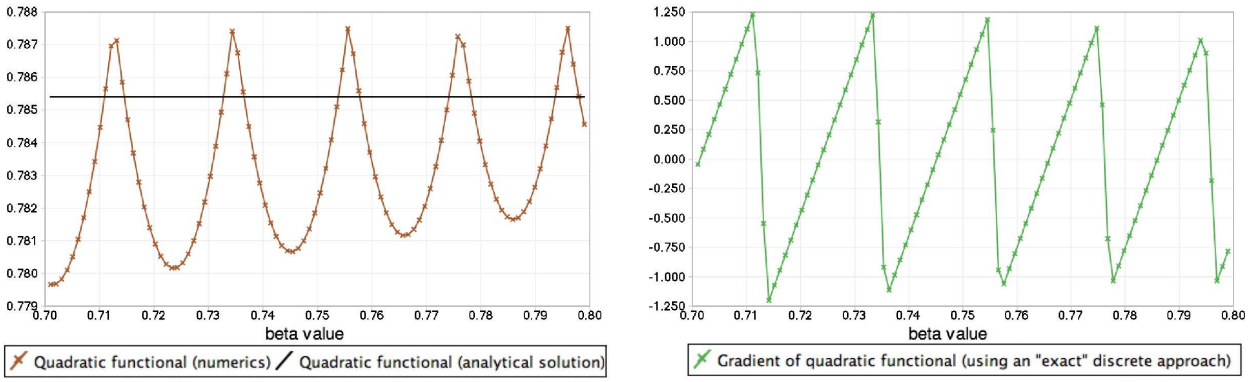

Figure 2. Analytical objective function vs. discrete objective function (left), and discrete gradient computed with a forward finite difference strategy.

where

$$U = \begin{pmatrix} \rho \\ \rho u \\ \rho E \end{pmatrix}, \quad F = \begin{pmatrix} \rho u \\ \rho u^2 + p \\ \rho u H \end{pmatrix}, \quad Q = \begin{pmatrix} 0 \\ p \\ 0 \end{pmatrix}. \tag{24}$$

Here, U represents the conserved variables, f is the convective flux vector, Q is the source vector, ρ is density, u is velocity, p is pressure, E is total energy and H is total enthalpy. The system is closed by the equation of state for an ideal gas

$$H = E + \frac{p}{\rho} = \frac{\gamma}{\gamma - 1}\frac{p}{\rho} + \frac{1}{2}u^2. \tag{25}$$

If the solution contains a shock at a point x_s, the Rankine-Hugoniot jump conditions connect the smooth solutions on either side of the shock. For steady flow the conditions can be written as:

$$[F(U)]_{x_s} = 0, \tag{26}$$

where $[z]_{x_s}$ denotes the jump of the quantity z at $x = x_s$ defined as $[z]_{x_s} = z(x_s^+) - z(x_s^-)$ and $z(x_s^-)$, $z(x_s^+)$ are the values of z to the left and right of the point $x = x_s$.

The problem under consideration consists on computing the gradient of the total pressure along the duct

$$J(\alpha) = \int_a^b p(x)dx. \tag{27}$$

with respect to variation on the duct height $h(x)$ which depends on some design parameters α that define its shape.

A. Objective function gradient using the continuous adjoint strategy

For steady flow we follow the derivation of Giles and Pierce.[10] We briefly outline the main results stated there. Consider the problem of minimizing the total pressure along the duct for a flow that has a shock wave located at the point $x = x_s$. Then, the objective function under consideration is:

$$J = \int_a^b p(x)dx = \int_a^{x_s} p(x)dx + \int_{x_s}^b p(x)dx \tag{28}$$

The classical adjoint approach starts by considering the flow equations, linearized with respect to variations in the design variables

$$\frac{d}{dx}\left(\delta h F(U) + h\frac{\partial F}{\partial U}\delta U\right) - \frac{d(\delta h)}{dx}Q - \frac{dh}{dx}\frac{\partial Q}{\partial U}\delta U = 0, \tag{29}$$

where δz is the variation of a quantity z due to a variation in the values of the design variables.

Equations (29) are then multiplied by a vector of adjoint variables $\Psi^T = (\psi_1, \psi_2, \psi_3)$. A new adjoint variable Ψ_s is introduced in order to enforce the (linearized) Rankine-Hugoniot conditions

$$\left[\frac{\partial F}{\partial U}\delta U\right]_{x_s} + \left[\frac{dF}{dx}\right]_{x_s} \delta x_s = 0. \tag{30}$$

Integrating by parts one obtains the expression for the gradient:

$$\begin{aligned}
\delta J &= \int_a^b \left(\frac{\partial p}{\partial U} - h\frac{d\Psi^T}{dx}\frac{\partial F}{\partial U} - \Psi^T \frac{dh}{dx}\frac{\partial Q}{\partial U}\right)\delta U\, dx \\
&- \int_a^b \left(\frac{d\Psi^T}{dx}\delta h F(U) + h\Psi^T \frac{d(\delta h)}{dx} Q\right) dx \\
&- h(x_s)\left(\Psi_s - \Psi(x_s^+)\right)^T \frac{\partial F}{\partial U}\delta U_{|x_s^+} + h(x_s)\left(\Psi_s - \Psi(x_s^-)\right)^T \frac{\partial F}{\partial U}\delta U_{|x_s^-} \\
&- \delta x_s \left(h(x_s)\Psi_s \left[\frac{dF}{dx}\right]_{x_s} + [p]_{x_s}\right).
\end{aligned} \tag{31}$$

In order to make vanish the boundary terms some restrictions are imposed on the adjoint variables. First, to eliminate the dependence on δU (i.e., the term on the third row of (31)) the condition

$$\Psi(x_s^+) = \Psi_s = \Psi(x_s^-) \tag{32}$$

is imposed. Next, from the last row of (31) the internal boundary condition at the shock

$$\psi_2(x_s) = -\frac{1}{\frac{dh}{dx}(x_s)} \tag{33}$$

is derived. Boundary conditions for the adjoint at the domain boundaries come from

$$\left[h\Psi^T \frac{\partial F}{\partial U}\delta U\right]_a^b = 0. \tag{34}$$

The value of δJ is then computed as

$$\delta J = -\int_a^b \left(\frac{d\Psi^T}{dx}\delta h F(U) + h\Psi^T \frac{d(\delta h)}{dx} Q\right) dx, \tag{35}$$

where Ψ is the solution of the adjoint equation

$$\frac{\partial p}{\partial U} - h\frac{d\Psi^T}{dx}\frac{\partial F}{\partial U} - \Psi^T \frac{dh}{dx}\frac{\partial Q}{\partial U} = 0. \tag{36}$$

Finally, it is important to mention that the continuous formulation can be solved analytically using Greens functions, so the solution is free from numerical errors.

B. Numerical tests in a supersonic nozzle

For this numerical test, the area of the nozzle is taken to vary as $h(x) = 1.05 + 0.07x + (0.04(x-5))^3$ in a domain of extent $x = [0., 10]$. The inlet Mach number is supersonic and the ratio of the exit pressure to the inlet pressure is set to be 2.5, resulting in a shock in the interior of the nozzle. The objective function J is taken to be the integral of pressure over the extent of the nozzle. The flow solution employs Roe's upwinding, and second order spatial accuracy (when used) is achieved using slope limited MUSCL schemes.[11]

Figure 3 compares the "discrete" derivative of the objective function with respect to the inlet Mach number with an "exact" or continuous adjoint procedure as detailed by Giles and Pierce.[10] The sawtooth-like structure of the gradient error is directly related to the resolution of the shock in the numerical solution. Small numerical errors (for instance, $< 0.0005\%$ for the second order scheme) in the flow solution appear to be greatly amplified in the gradient computation as seen in Figure 4.

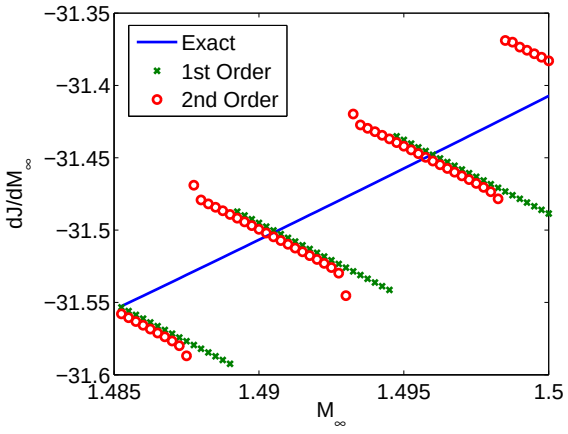

Figure 3. Functional gradient computed with the discrete adjoint method using Roe upwinding

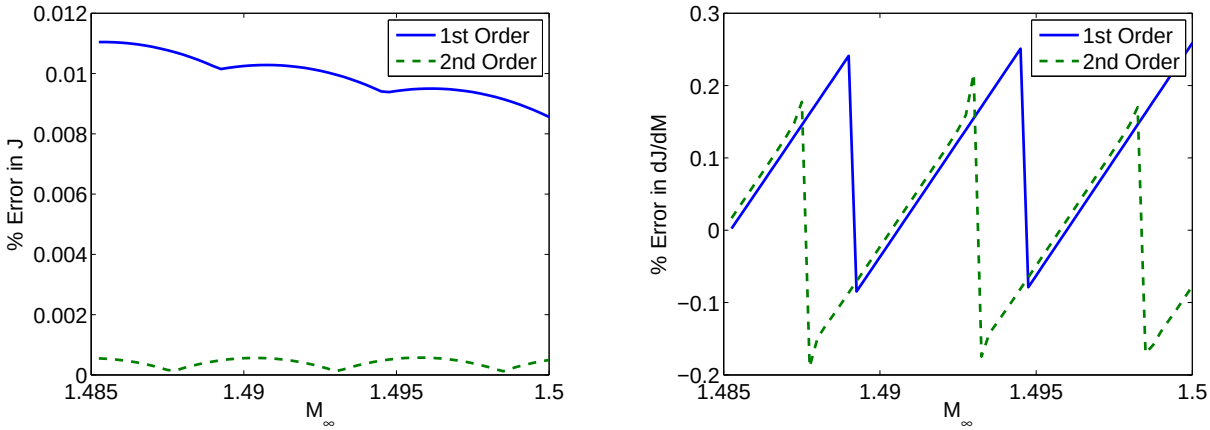

Figure 4. Functional (left) and functional gradient (right) computed with the discrete adjoint method using Roe upwinding

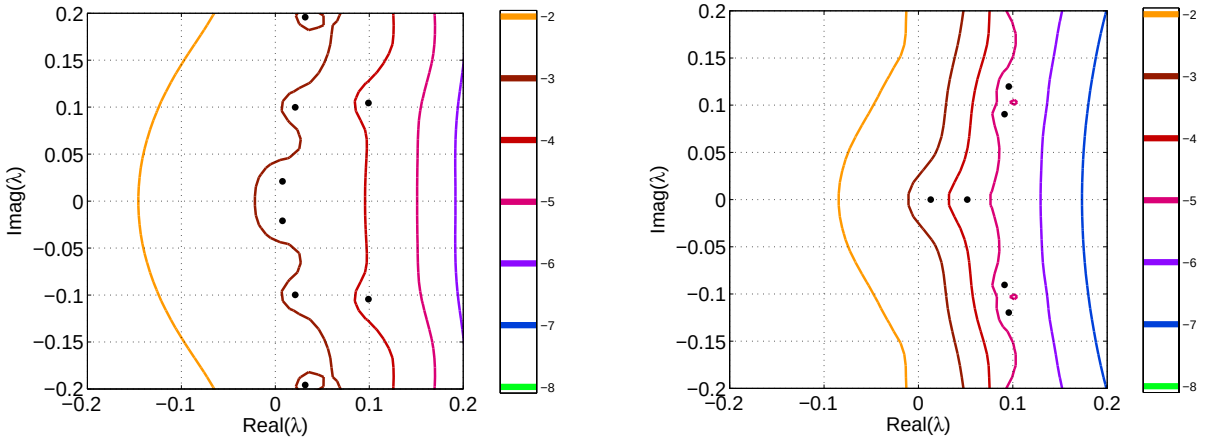

Figure 5. Eigenvalues and pseudospectral contours (of the global Jacobian matrix) corresponding to 1st order Roe upwinding for Quasi-1D nozzle. Left: $M_\infty = 1.494606$, Right: $M_\infty = 1.494607$

The cyclical nature of the error is due to the shock location crossing grid cells. It has to be recognized that when the shock is positioned at the interface, the Roe's scheme results in perfect shock capturing by excluding artifical dissipation locally. This is ensured by the fact that one wave speed ($u_{Roe} - c_{Roe}$) and two wave amplitudes (corresponding to u_{Roe} and $u_{Roe} + c_{Roe}$) assume zero values. Such a balance is lost, however, when the captured shock position deviates from the cell interface by the slightest amount, resulting in the addition of local artificial dissipation.

Further, the dissipation term typically involves absolute values that introduce discontinuities in the differentiation chain during the linearisation process. Figure 5 shows the spectra and pseudo-spectra of the global Jacobian matrix near the origin for the first order Roe upwinding scheme. While the differences in the flow solutions between the two cases cannot be distinguished clearly, the topological difference in the eigenstructure is obvious. $M_\infty = 1.494607$ corresponds to a case of near-perfect shock capturing, whereas $M_\infty = 1.494606$ results in a very small deviation of the shock to the left of the interface.

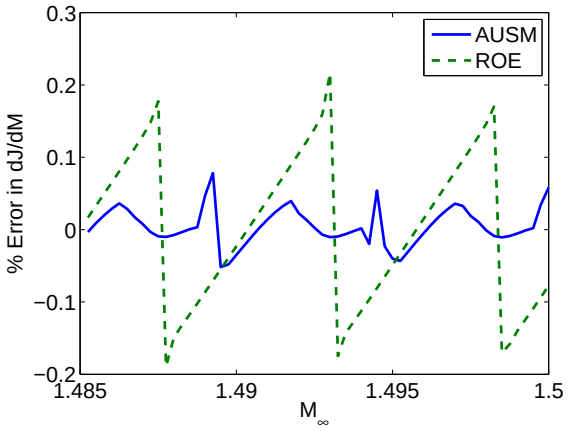

Figure 6. Functional gradient computed with the discrete adjoint method using Roe and AUSM based upwinding

The numerical noise in the gradient was seen to maintain its basic character but reduced by a factor of half in amplitude with mesh refinement. As shown in Figure 6, the noise is also present for other upwind schemes.

Thus, while the discrete adjoint gives exact discrete sensitivities and does not require explicit provision of adjoint Rankine-Hugoniot boundary conditions at discontinuities, numerical noise is to be expected in gradient computations and could potentially be $\mathcal{O}(1)$ in the presence of strong shocks. The adverse effects of this noise could potentially be reduced by adding additional numerical dissipation near discontinuities, as suggested in,[7] or by filtering the solution, as proposed by.[8] Alternatively, shock fitting could prove to be beneficial.

IV. Systems governed by the 2D Euler's equations

Ideal fluids are governed by the Euler's equations, which express the conservation of mass, momentum (with null viscosity) and energy. The most common way to pose the 2D Euler's equations is in conservative form:

$$\begin{cases} \partial_t U + \vec{\nabla} \cdot \vec{F} = 0, & \text{in } \Omega, \\ \vec{v} \cdot \vec{n}_S = 0, & \text{on } S, \end{cases} \tag{37}$$

where $\vec{n}_S$ is an inward-pointing unit vector normal to S, and at the "far field", boundary conditions are specified for incoming waves, whereas outgoing waves are determined by the solution inside the fluid domain.

The conservative variables are $U = (\rho, \rho v_x, \rho v_y, \rho E)^T$ and $\vec{F} = (F_x, F_y)$ is the convective flux vector

$$F_x = \begin{pmatrix} \rho v_x \\ \rho v_x^2 + P \\ \rho v_x v_y \\ \rho v_x H \end{pmatrix}, \quad F_y = \begin{pmatrix} \rho v_y \\ \rho v_x v_y \\ \rho v_y^2 + P \\ \rho v_y H \end{pmatrix}, \tag{38}$$

where ρ is the fluid density, $\vec{v} = (v_x, v_y)$ is the flow velocity in a Cartesian system of reference, E is the total energy, P the system pressure and H the enthalpy. As in the quasi 1D problem, the system of equations (37) must be completed by an equation of state which defines the thermodynamic properties of the fluid.

A. Objective function gradient using the continuous and discrete adjoint strategy

In optimal shape design the adjoint formulation is introduced to compute the gradient of an objective function (2). If a continuous approach is used, the adjoint problem is introduced[12] through the Lagrange multipliers $(\Psi^T) = (\psi_1, \psi_2, \psi_3, \psi_4)$ which satisfy the following adjoint system:

$$\begin{cases} -\vec{A}^T \cdot \vec{\nabla}\Psi = 0, & \text{in } \Omega \setminus \Sigma, \\ \vec{\varphi} \cdot \vec{n}_S = \partial j / \partial U, & \text{on } S \setminus x_s, \\ \Psi^T \left(\vec{A} \cdot \vec{n}_{\Gamma_\infty} \right)_- = 0, & \text{on } \Gamma_\infty, \\ \left[\Psi^T \right]_\Sigma = 0, \quad \partial_{tg} \Psi^T \left[\vec{F} \cdot \vec{t}_\Sigma \right] = 0, \quad L = \Psi|_\Sigma, & \text{on } \Sigma, \\ \Psi^T(x_s) \left[\vec{F} \cdot \vec{t}_\Sigma \right]_{x_s} = [j]_{x_s} / \left(\vec{n}_s \cdot \vec{t}_\Sigma \right), & \text{at } x_s, \end{cases} \tag{39}$$

where $\partial \vec{F} / \partial U = \vec{A}$, and $\partial_n = \vec{n} \cdot \vec{\nabla}$ and $\partial_{tg} = \vec{t} \cdot \vec{\nabla}$ are the normal and tangential derivatives (respectively), x_s is the shock location, and $\vec{\varphi} = (\psi_2, \psi_3)$. Finally, the objective function variation is computed as:

$$\begin{aligned} \delta J(S) &= \int_{S \setminus x_s} \left[\partial_n j(P) + \vec{t} \cdot \partial_{tg} \left(\frac{\partial j}{\partial \vec{n}_s} \right) - \kappa \left(j + \frac{\partial j}{\partial \vec{n}_s} \vec{n}_s \right) \right] \delta S \, ds \\ &+ \int_{S \setminus x_s} \left[\left(\partial_n \vec{v} \cdot \vec{n}_S \right) \vartheta + \partial_{tg} \left(\left(\vec{v} \cdot \vec{t}_S \right) \vartheta \right) \right] \delta S \, ds \\ &+ [j(P)]_{x_s} \frac{\vec{n}_S \cdot \vec{n}_\Sigma}{\vec{n}_S \cdot \vec{t}_\Sigma} \delta S(x_s) - \vec{t} \cdot \left[\frac{\partial j}{\partial \vec{n}_S} \right]_{x_s} \delta S(x_s). \end{aligned} \tag{40}$$

where κ is the curvature, and $\vartheta = \rho\psi_1 + \rho \vec{v}_S \cdot \vec{\varphi} + \rho H \psi_4$. Using (39) and (40) we are able to solve any shape design problem with the Euler's equations, and we will use this methodology to compute the continuous gradient value in the numerical experiment that will be presented in this section.

With respect to the "discrete" gradient computation, we will use a forward difference approximation in which the value of the first-order derivative is computed as

$$\frac{\partial J_{\Delta x}}{\partial S} = \lim_{\delta S \to 0} \frac{J_{\Delta x}(S + \delta S) - J_{\Delta x}(S)}{\delta S}, \tag{41}$$

where an especial care must be taken in the calibration of δS, which must be greater than the machine precision, but small enough to provide the "exact" discrete gradient.

B. Numerical tests of optimal shape design

The aim of this section is to identify numerical oscillations introduced by the discretization of the discontinuities and its effect in the gradient calculation using an "exact" discrete approach.

In this 2D problem it is fair to mention that the evaluation of objective functions using computational grids that are not well oriented provides also oscillatory results at some small scales. This is, typically, a multidimensional problem, in which the computational grid introduces some numerical error because it is not aligned with the shock waves.

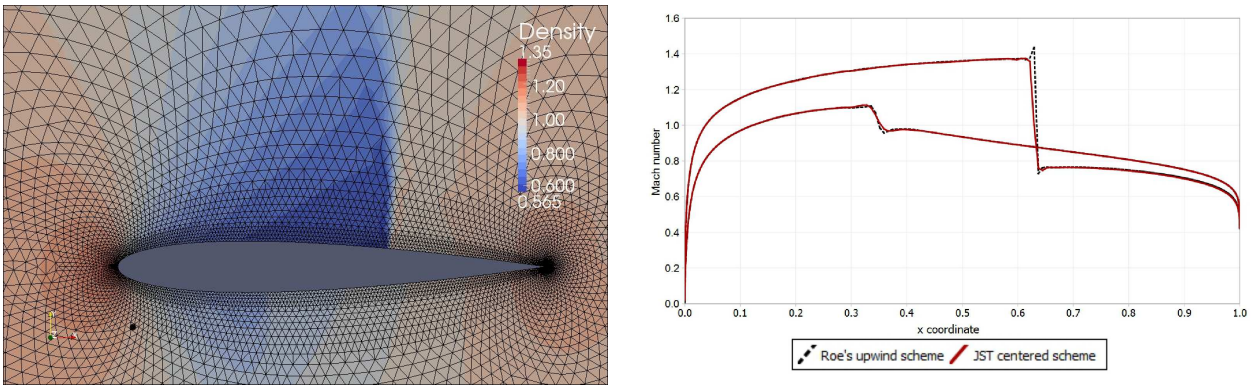

Figure 7. Density field on the finest grid (left) and air velocity on the surface for both grids (right).

As baseline we have chosen a NACA 0012 airfoil, with transonic flow conditions (angle of attack 1.25°, Mach number 0.8). Gradients of the cost function are obtained with respect to 50 Hicks-Henne sine "bump" functions,[5] centered at various locations along the upper surfaces of the baseline airfoil.

Regarding the spatial discretization, two computational grids of 5233 (coarse grid) and 7908 points (fine

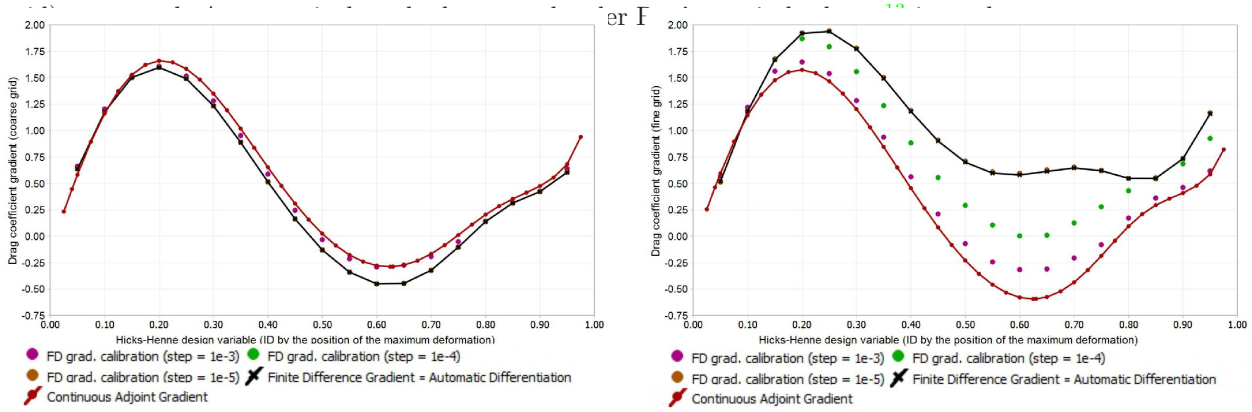

Figure 8. Comparison of $\vec{\nabla} J_{\Delta x}$ computed with a Finite Difference strategy (the step calibration is also shown), with $\vec{\nabla} J$ computed using a continuous adjoint methodology.

The first step is the calibration of the finite difference step. Then, the "exact" discrete gradient will be compared with the "continuous" gradient or "exact" analytical gradient (in a hypothetical case in which we don't have any numerical error). In figure 8 we have plotted the discrete and the continuous gradient for both computational grids. It is important to highlight that in the coarsest grid the continuous and the discrete gradient provides similar results, however in the finest grid there is a relevant difference between both approaches.

The next test consists in studying the behavior of $J_{\Delta x}$ when only a design variable on the shock location is used. In figure 9 both objective functions are compared. Note that for the drag coefficient computation they are some local minimums.

In this section we have checked that in a 2D Euler transonic case high frequency fluctuations may appear in the objective function evaluation when the appropriate design variable is chosen. If that situations happens in a optimization process, and nothing is done, they there are two possibilities:

- If our optimization algorithm is good enough (the optimization step is well selected), a local minimum will be found, but this minimum could be far away from the global minimum of our problem.
- If the step of the optimization algorithm is not adequate (larger than validity zone of the first derivative), we will not find the local minimum, neither a global one.

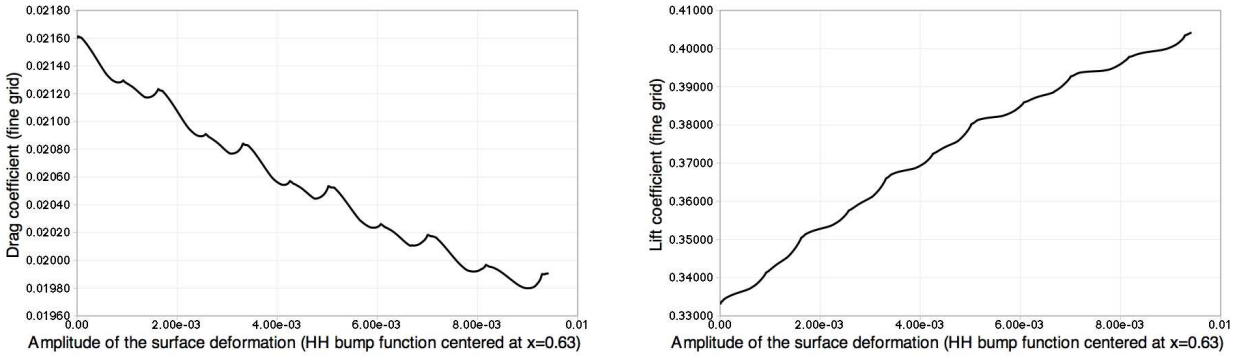

Figure 9. Drag and lift coefficient computation for a design variable located at the shock position using the finest grid.

Finally, two optimization problem will be introduced in order to show the relevance of the phenomena that we have described in the previous paragraphs. As design variables we will use several Hicks-Henne bump located at strategics points. In the sake of simplicity the objective function will be the drag coefficient (without any kind of constrains). As optimization algorithm a Broyden-Fletcher-Goldfarb-Shanno (BFGS) optimization method[14] is used.

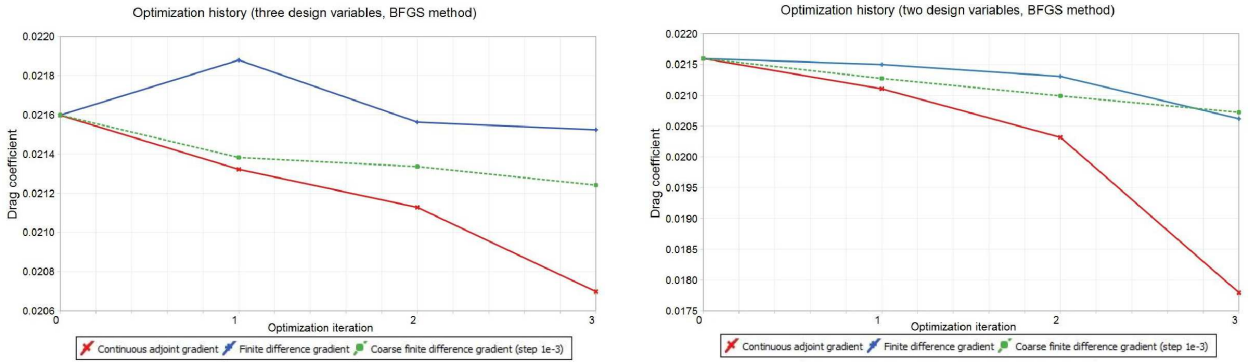

Figure 10. Optimization history for a problem with 3 design variables (left) and 2 design variables (right)

Figure 10 (left) shows the optimization history of the problem with three design variables (centered at position 0.53, 0.63 –shock wave location–, 0.73). In that figure it is possible to compare the optimization using an "exact" discrete gradient strategy, a continuous adjoint method ("exact" analytical method), and a non-exact discrete gradient strategy (finite differences with a coarse finite step). In this case, it is clear that the "exact" discrete gradient is not efficient. A continuous adjoint strategy or even a finite difference strategy with a coarse step provides better results than the "exact" discrete gradient.

We will take advantage of this problem to define the "physical relevance amplitude" as the minimum amplitude of the design variable which produces a change in the objective function greater than the order of the numerical method. Below this threshold, the changes in the objective function are mainly due to adjustments in the artificial dissipation introduced by the numerical scheme. Related with this concept, in Figure 10 (right), we pose another optimization problem in which the design variables are 2 bump function centered at position 0.04 (sonic point), 0.63 (shock location point). As before, 3 different strategies are plotted for computing the gradient. Note that we are putting together two design variables with a very different "physical relevance amplitude" (first order of accuracy for the point located at the shock and second order for the point located at the sonic point), and the optimization using "exact" discrete approach is again not efficient.

V. Conclusions

Throughout this article we have checked that the way in which the shock wave is discretized can have a relevant influence in a optimal shape optimization process. Even more, we have establish the "physical relevance amplitude", which provides a hint about which design variables can be used together in a optimization problem. This is important because if we mix design variables with different "physical relevance amplitudes" the optimization algorithm will not work properly.

It is also important to stress that the Automatic Differentiation (AD) techniques provides the "exact" discrete gradient. However, that gradient could be dominated, at the smallest scales, by the particular discretization of the discontinuity. In that scenario, the "exact" discrete gradient only represents the behavior of $J_{\Delta x}$ for very small (non-physical or below the "physical relevance amplitude") modifications of some relevant design parameter.

As conclusions of this article it is possible to give some basic recipes in order to obtain a successful descend direction dealing with shocked flows:

- Use, if available, the continuous strategy for computing the gradient of the objective function.
- If the continuous adjoint is not available, it is important to apply some filtering techniques to eliminate the numerical fluctuations of the discrete functional or add some additional smooth numerical dissipation near discontinuities.
- If an Automatic Differentiation is available, then it is better to apply the technique on a coarse grid, where we have interpolated the flow solution obtained in a finest grid (bi-grid strategy). This is equivalent to do a smoothing of the flow solution.
- Do not introduce the nodes that are inside the discrete representation of the shock in the objective function evaluation.
- Do not mix in a optimization process design variables with different "physical relevance amplitudes".
- If possible, always use design variables which provide a linear relationship between the objective function and the deflection of the surface.
- To avoid orientation effects, use hp-adaptation or a structured numerical grid.

Those are very easy recipes that should improve the convergence of an optimal shape optimization problem when dealing with shocked flows.

Acknowledgments

The research described in this paper has been supported under the FuSim-E Programme funded by Airbus Spain. Also, this work has been partially supported by the project MTM2008-03541 of the Spanish MIICIN and the ERC Advanced Grant NUMERIWAVES.

References

[1]Jameson, A., "Aerodynamic design via control theory," *Journal of Scientific Computing*, Vol. 3, No. 9, 1988, pp. 233–260.

[2]Castro, C., Lozano, C., Palacios, F., and Zuazua, E., "A systematic continuous adjoint approach to viscous aerodynamic design on unstructured grids," *AIAA Journal*, Vol. 45, No. 9, 2007, pp. 2125–2139.

[3]Nadarajah, S. and Jameson, A., "A Comparison of the Continuous and Discrete Adjoint Approach to Automatic Aerodynamic Optimization," Aiaa paper 2000–0667, American Institute of Aeronautics and Astronautics, Jan. 2000.

[4]Mader, C. A., Martins, J. R. R. A., Alonso, J. J., and van der Weide, E., "ADjoint: an approach for rapid development of discrete adjoint solvers," *AIAA Journal*, Vol. 46, No. 4, 2008, pp. 863–873.

[5]Hicks, R. M. and Henne, P. A., "Wing Design by Numerical Optimization," *Journal of Aircraft*, Vol. 15, No. 7, 1978, pp. 407–412.

[6]Martins, J. R. R. A., Sturdza, P., and Alonso, J. J., "The complex-step derivative approximation," *ACM Transactions on Mathematical Software*, Vol. 29, No. 3, 2003, pp. 245–262.

[7]Giles, M. B., Duta, M. C., Müller, J.-D., and Pierce, N. A., "Algorithm Developments for Discrete Adjoint Methods," *AIAA Journal*, Vol. 41, No. 2, 2003, pp. 198–205.

[8]Palacios, F., Duraisamy, K., and Alonso, J. J., "A Comparison of the Continuous and Discrete Adjoint Approach to Automatic Aerodynamic Optimization," Ctr annual research briefs, Center for Turbulence Research, NASA Ames/Stanford University, Dec. 2009.

[9]Chen, Q.-Y., Gottlieb, D., and Hesthaven, J. S., "Uncertainty analysis for the steady-state flows in a dual throat nozzle," *Journal of Computational Physics*, Vol. 204, No. 1, 2005, pp. 378–398.

[10]Giles, M. and Pierce, N., "Analytic adjoint solutions for the quasi-one-dimensional Euler equations," *Journal of Fluid Mechanics*, Vol. 426, 2001, pp. 327–345.

[11]van Leer, B., "Towards the Ultimate Conservative Difference Scheme, V. A Second Order Sequel to Godunov's Method," *Journal of Computational Physics*, Vol. 32, 1979, pp. 101–136.

[12]Baeza, A., Castro, C., Palacios, F., and Zuazua, E., "2-D Euler Shape Design on Nonregular Flows Using Adjoint Rankine-Hugoniot Relations," *AIAA Journal*, Vol. 47, No. 3, 2009, pp. 552–562.

[13]Roe, P. L., "Approximate Riemann Solvers, Parameter Vectors, and Difference Schemes," *Journal of Computational Physics*, Vol. 43, No. 2, 1981, pp. 357–372.

[14]Broyden, C. G., "The Convergence of a Class of Double-rank Minimization Algorithms 1. General Considerations," *IMA Journal of Applied Mathematics*, Vol. 6, No. 1, 1970, pp. 76–90.